sustainability

MDPI

Article

Within-Class and Neighborhood Effects on the Relationship between Composite Urban Classes and Surface Temperature

Peleg Kremer [1,*], Neele Larondelle [2], Yimin Zhang [3], Elise Pasles [3] and Dagmar Haase [4]

1 Department of Geography and the Environment, Villanova University, Villanova, PA 19085, USA
2 Institute of Geography, Humboldt Universität zu Berlin, 10099 Berlin, Germany; neele.larondelle@europarc-deutschland.de
3 Department of Mathematics and Statistics, Villanova University, Villanova, PA 19085, USA; yimin.z@villanova.edu (Y.Z.); elise.pasles@villanova.edu (E.P.)
4 Department of Computational Landscape Ecology, Institute of Geography and Helmholtz Centre for Environmental Research—UFZ, Humboldt Universität zu Berlin, 10099 Berlin, Germany; dagmar.haase@ufz.de
* Correspondence: peleg.kremer@villanova.edu; Tel.: +1-610-51945449

Received: 27 December 2017; Accepted: 24 February 2018; Published: 28 February 2018

Abstract: Understanding the relationship between urban structure and ecological function—or environmental performance—is important for the planning of sustainable cities, and requires examination of how components in urban systems are organized. In this paper, we develop a Structure of Urban Landscape (STURLA) classification, identifying common compositions of urban components using Berlin, Germany as a case study. We compute the surface temperature corresponding to each classification grid cell, and perform within-cell and neighborhood analysis for the most common composite classes in Berlin. We found that with-class composition and neighborhood composition as well as the interaction between them drive surface temperature. Our findings suggest that the spatial organization of urban components is important in determining the surface temperature and that specific combinations, such as low-rise buildings surrounded by neighborhood trees, or mid-rise buildings surrounded by high-rise buildings, compound to create a cooling effect. These findings are important for developing an understanding of how urban planning can harness structure-function relationships and improve urban sustainability.

Keywords: urban structure; STURLA; surface temperature; urban sustainability; urban composition; urban ecosystem services

1. Introduction

Urbanization is a core process affecting our ability to address the local and global challenges of sustainability. The scope and pace of urbanization are described extensively in the literature. It is by now clear that urban sustainability is among the most important global challenges of our era [1]. A determinant feature of such urban areas is their spatial heterogeneity and the disturbance they cause to natural processes. Recent literature on urban ecosystem services (ES) [2] and urban ecology [3] highlights the importance of natural processes within cities and the ways in which they benefit human wellbeing. Understanding cities as integrated human-nature systems can support the development of sustainable urban solutions [4]. However, for urban planners to be able to integrate ecological principles in planning practices requires both a better understanding of the relationship between urban structures and ecological phenomena, and the translation of this understanding into tools that can be easily integrated into decision making processes. Urban spatial structure is

important in understanding urban ES provision, and it can provide a bridge to planning sustainable cities [5]. Urban structure characteristics—including vegetation and other land covers—can be used to estimate ecological functions [6,7]. However, defining urban structures—and key relationships between urban structures—and ecological processes is especially challenging in landscapes characterized by density and patchy spatial patterns [8]. A functional classification of urban structure is necessary for understanding the nature of social-ecological relationships in urban areas [3,9,10]. The Structure of Urban Landscape (STURLA) classification system was developed to provide a simple, unbiased, multi-dimensional classification of urban land covers, their composition, and neighborhood structures. In previous papers [11,12], we outlined the rationale of STURLA and presented initial case studies in Berlin and New York City (NYC). The premise of the classification is that the relationship between urban structure and ecological function/environmental performance, requires an examination of the complexity of urban structure, in particular how components within urban systems are organized. Particularly important is the vertical dimension, which, thus far, is rarely addressed [13,14]. To achieve an unbiased approach to urban structure classification, Hamstead et al. [11] developed a procedure that depends on fusing fine scale urban land cover with building height information and overlaying this with a classification grid cell of a predetermined scale. Each cell in the classification grid is characterized by a combination of the components that fall within that cell. Different classification units and scales were tested, along with their relationship to one biophysical function that is important for human health in cities: urban surface temperature.

The mechanisms by which urban atmospheric temperatures differ from non-urban regions are complex and relate to urban structures and human activity [15]. Oke [16] describes the main ways by which urban landcover and land use influence temperatures. In essence, human-made structures and surfaces alter the natural balance of surface energy and radiation through mechanisms such as: absorption of radiation by vertical surfaces; retention of infrared radiation in street canyons; uptake and retention, or delayed release of heat by buildings and paved surfaces; conversion of solar radiation to sensible heat rather than latent heat due to decline in surface transpiration; and the release of sensible and latent heat from the combustion of fuels related to urban activities [15,16]. Thus, analyzing urban structures for these mechanisms, including the adsorption by vertical dimensions is critical for understanding temperature patterns across urban areas. Remotely sensed surface temperatures have been used in diverse ways: as an indicator of environmental performance and a proxy of multiple ecological processes in urban systems [17,18] to support the development of an urbanization index [19], to study its relationship to land cover [20]; as an urban heat island [21–25]; and for urban structures and configurations [24–29]. Studying the surface temperature of different green spaces, Chen et al. [30] found that configurations such as edges, shape, size, and connectivity, are correlated with surface temperature and that this relationship varies over different types of green surfaces. Some studies focus only on the difference in surface temperature between green and impervious surfaces [22,24,25], while other studies consider more specific urban landcovers [21,28] or combine measures of vegetation with demographic and socioeconomic variables [21,26]. A remotely sensed surface temperature is an appealing indicator because specific data is available at a rare combination of conditions continuous spatial coverage and at both moderate spatial and temporal resolution. This thus allows for analysis of variations within urban systems. Few other indices or proxies are available that provide all three of these necessary characteristics. Findings commonly associate the occurrence of vegetation and vegetation density with cooler temperatures than when associates with paved surfaces.

In previous research using STURLA, empirical evidence from two cities—Berlin and NYC—suggest that it is possible to identify common urban structure units that encompass the majority of the cities' land area, at least in the case study examples from the western world [12]. Moreover, when correlated to surface temperature, these common urban structure classifications exhibit distinct temperature signatures for different urban structure units with temperature trends dramatically similar between Berlin and NYC [11,12]. These results suggest the potential to transform our understanding of the relationship between urban structure and ecological function, but they require further study to

expand the classification system—to new geographic locations, ecological functions and environmental performance indicators and to verify their stability across scales and test the initial results from the cited papers.

Although previous research showed a clear distinction between the temperature signatures of most of the composite classes, it also showed a large variability in temperature within certain (mixed) classes. This variability may be due to both a local (within cell) and a neighborhood effect of urban land unit composition on surface temperature [12].

In this paper, we continue to explore STURLA classification as it relates to surface temperature. Here, however, we examine the surface temperature variability within the most common composite class in Berlin. This class is examined as a function of the proportion of the individual components in the class (within-class influence) and of neighborhood influence. We hypothesize that the variation in temperature may be influenced by the proportion of the different land cover components in and around the grid cell, and that the influence of some components will show a stronger effect from neighborhood parameters (for example trees) while other components will show stronger local effects (low buildings).

Therefore, the main research questions in this paper are:

- Within STURLA classes, which land cover class components have the most significant impact on surface temperature?
- What are the neighborhood effects on surface temperature?
- How do land cover components and neighborhood effect interact in driving the surface temperature of particular STURLA classes?

Testing the classification system to understand the quantitative influence of the individual components will help test the basic STURLA assumption that we can use a simple present/absent test to determine urban composite classes. Understating the drivers behind the relationship between surface temperature and classification components will also strengthen the classification method by testing the importance of each of the different urban components in determining surface temperature and by suggesting any potential neighborhood effect that might guide further scale considerations classification and analysis.

2. Methods

2.1. The Case Study of Berlin

Berlin has a population of about 3.5 million within an area of about 900 sq km. In comparison to other European cities that have more than 500,000 inhabitants, Berlin is ranked 23rd in terms of population density. Open and green spaces comprise 45% of Berlin's land use, the majority of which is forested. The amount of green space increases with distance from the city center. However, the presence of large urban green spaces of more than two sq km in inner-city areas is a unique feature of Berlin. Built-up areas represent 55% of Berlin's land use. About half of the built-up area is residential and most residential areas are made up of low-rise buildings. A midrise building structure composed of what are typical five-story Wilhelminian buildings, forms a ring around the city center. High-rise buildings can be found within the dense city center or elsewhere locally on locations of prefabricated high-rise residential buildings [12]. The city of Berlin is used as a case study here to present a continuation of previous STURLA research. In addition, Berlin's land use and landscape structures are representative in terms of the area's building stock erected continuously from the times of early industrialization in the 1850s until today. Also, population densities in the high-, mid- and low-rise buildings are typical of Germany and other Central European cities [31,32] so that findings for Berlin are representative of at least Central European cities. Moreover, Berlin offers a great variety of built and non-built neighborhoods to extensively test the STURLA-approach. Berlin had been used as a sample city for many similar social-ecological studies and, thus, the results we show in this paper can be compared to and contextualized by this body of knowledge.

2.2. Berlin Classification and Class Grass/Shrubs (g) –Tree Canopy (t) –Low-Rise (l) –Mid-Rise (m) –Roads-Other Paved (p) –Bare Soil (b) (GTLMPB)

To create the STURLA classification we used an integrated land cover and building dataset that was overlaid with the classification grid of 120 sq m. This study improves on Larondelle et al. [12] by creating a new integrated dataset utilizing previously unavailable, high resolution data from Berlin's Environmental Atlas [33,34]. The new building and vegetation height dataset, derived from high resolution, multispectral airborne imagery using varying segmentation methods [34] was integrated with a dataset on soil sealing [33]. Subsequently [35], we categorized a height of five meters and above as tree cover and below five meters vegetation as grass/shrub cover. The building height dataset was classified as low-rise (1–3 stories), mid-rise (4–9 stories) and high-rise (above 9 stories). Roads and water classes were created using roads and water layers from the Urban Atlas [36]. Surface sealing data from the Environmental Atlas Berlin [33] was used to distinguish between bare soil and other paved land covers. First, all pixels with no vegetation and a sealing rate of 0 were reclassified as bare soil. Pixels with a sealing rate higher than 0, which could not be classified using other input data as building or roads were reclassified as other paved. Next, the five raster datasets (building, tree canopy/grass-shrubs, roads, water, and other paved/bare soil) were resampled into aligning 2.5 m raster and were mosaicked to create an interceded dataset that includes the following classes: trees, grass/shrub, bare soil, water, low-rise, mid-rise, high-rise, roads and other paved surfaces. Finally, roads and other paved surfaces classes were collapsed into one class and termed "paved".

All data we have used for the city of Berlin has been based on data collected around the year 2010. For this reason, the surface temperature data was selected from 2010. All GIS analyses in this study were performed using ESRI ArcGIS 10.3.1 (ESRI, Redlands, CA, USA).

The integrated dataset was overlaid with a classification grid of 120 sq m. Each grid cell was assigned a STURLA class by identifying and concocting all urban components present within the grid cell [11]. Next, we identified the most common STURLA class as class 'GTLMPB' –grass/shrubs (g) –tree canopy (t) –low-rise (l) –mid-rise (m) –roads-other paved (p) –bare soil (b), which covers 35% of the total area of Berlin. GTLMPB pixels were extracted for further analysis.

2.3. Within-Class and Neighborhood Analysis

Within-class Composition. We derived the percent cover of all components within each classification grid cell in the 'GTLMPB' class by running the Zonal Analysis tool 'Zonal Statistics as Table'. In ArcGIS, Zonal Statistics allows the calculation of a particular statistic (such as min, max or mean) for each zone in a zone database, using values from another dataset. Here the classification grid serves as the zone dataset and the landcover dataset is used to calculate the proportion of different landcovers within each zone (grid cell).

Neighborhood Composition. We used the results from the zonal analysis described above to assign a percent value to each STURLA cell for each urban component in the study area. We then computed the mean of each component in neighboring cells using the 'Focal Statistics' tool. Neighborhood was defined as the immediate adjacent STURLA cells to each 'GTLMPB' cell (a 3×3 matrix) and excluding the cell itself. Figure 1 illustrates the within-cell and neighborhood analysis concepts.

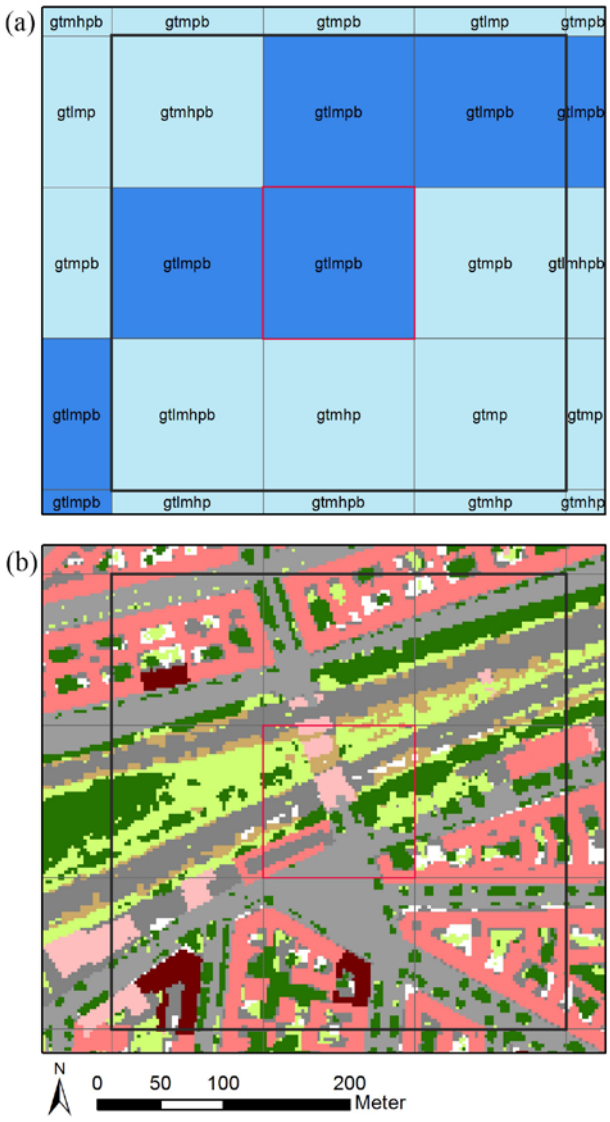

Figure 1. Same data frame from the Berlin map; (**a**) the classification cells with their different classes (above); (**b**) with fused land cover and building height underlying data in the background (below).

2.4. Surface Temperature

The surface temperature was obtained from the Landsat thermal band 6(1). We obtained monthly composite data for the month of July 2010 from the Global Web-enables Landsat Data (WELD) website. WELD data is terrain-corrected and radiometrically calibrated Landsat data [37]. There are known uncertainties associated with utilizing temporally composite surface temperature datasets [38]. However, Landsat 7 scanline error and resulting data gaps means that a composite of at least two scenes is necessary. WELD compositing procedures rely on an hierarchical pixel by pixel decision rationale documented by Roy et al. [39].

As the basis for surface temperature we used the WELD top of the atmosphere brightness temperature. We converted the top of the atmosphere brightness temperature to surface temperature using the following equation [22,25]:

$$ST = \frac{T_B}{1 + \left(\lambda \times \frac{T_B}{\rho}\right) \ln(\varepsilon)} \quad (1)$$

where ST = surface temperature (C); T_B = brightness temperature obtained from WELD; λ = wavelenth of emitted radiance (11.5 μm) $\rho = h \times c/\sigma = 1.438 \times 10^{-2}$ mK (σ = Boltzmann constant = 1.38×10^{-23} J/K, h = Planck's constant = 6.626×10^{-34} Js, c = velocity of light = 2.998×108 m/s; ε = land surface emissivity.

Land surface emissivity was estimated based on landcover properties and on NDVI [25,40–42]. We used the NDVI layer obtained from WELD [39] based on the same composite data as the thermal data. An NDVI greater than 0.5 was assumed to have an emissivity of 0.99. The emissivity of pixels with NDVI values between 0.2–0.5 were calculated as:

$$\varepsilon = \varepsilon_v \times P_v + \varepsilon_s(1 - P_v) \quad (2)$$

where ε_v = emissivity of vegetation (0.99), ε_s = emissivity of soil (0.97). P_v was calculated as follows [42]:

$$P_v = \left(\frac{\text{NDVI} - \text{NDVI}_{\text{min}}}{\text{NDVI}_{\text{max}} - \text{NDVI}_{\text{min}}}\right)^2 \quad (3)$$

Pixels with NDVI < 0.2 were assigned an emissivity of 0.97 [42]. Finally, LANDSAT cloud classification was obtained through WELD and pixels suspected as clouds were removed from the image.

2.5. Analysis of Relationship between Surface Temperature and Within-Class and Neighborhood Variables

To investigate the relationship between surface temperature and within-class and neighborhood variables, we developed a least squares regression model, with surface temperature as the response variable and percentage covers of urban components (within-class and neighborhood) as potential explanatory variables (see Table 1).

Table 1. Variable description.

Var.	Var. Description	Var.	Var. Description
ST	Surface temperature (°C)	NH_1	% neighborhood grass/shrub cover
IC_1	% within-class grass/shrub cover	NH_2	% neighborhood tree cover
IC_2	% within-class tree cover	NH_3	% neighborhood low-rise cover
IC_3	% within-class low-rise cover	NH_4	% neighborhood mid-rise cover
IC_4	% within-class mid-rise cover	NH_5	% neighborhood high-rise cover
IC_6	% within-class road cover	NH_6	% neighborhood road cover
IC_8	% within-class bare soil cover	NH_7	% neighborhood water cover
IC_9	% within-class other paved cover	NH_8	% neighborhood bare soil cover
		NH_9	% neighborhood other paved cover

Figure 2 shows our overall statistical modelling scheme for analyzing the data. The details are included in the following four major steps.

2.5.1. Data Exploration

First, we explored data and removed the observations where there were missing surface temperatures. Then the Box-Cox transformation [43] was applied on the response variable to correct non-normality and/or non-constant variance, which are major violations of regression assumptions. In the final model, the power transformation y^{-2} was found to be the appropriate transformation. Hence $1/ST^2$ was used as the response variable. The later step of model diagnostics showed that this transformation made large improvements in model fit.

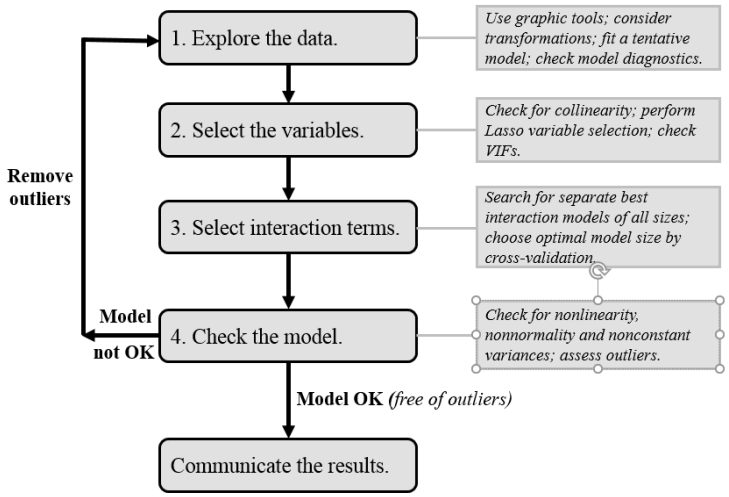

Figure 2. Strategy diagram for data analysis.

2.5.2. Variable Selection

The preliminary exploration of the relationship between surface temperature and model variables is presented in Appendix A as a matrix of plots with bivariate scatterplots below the diagonal, histograms on the diagonal, and the Pearson correlation coefficients above the diagonal. The figure shows that high correlation occurs in the same urban components for within-class and neighborhood variables, which is to be expected, as well as across components, such as NH_2 & NH_9 and NH_1 & NH_4. All of these suggest a problem of multicollinearity. Due to the multicollinearity issue in the data, we used the Lasso method [44] to perform variable selection—that is, to exclude irrelevant and highly correlated explanatory variables from the regression model. The variance inflation factor (VIF) [45] is an important assessment of the severity of the collinearity problem. A large VIF value may indicate a serious collinearity problem. Thus, we adjusted the tuning parameter in the Lasso selection to remove enough irrelevant variables such that the VIFs of all the remaining variables in the model were controlled under 5.

2.5.3. Interaction Terms Selection

In addition to the individual explanatory variables, we were also interested in the meaningful interactions among the explanatory variables to see if these interactions could further contribute to the model. We selected the best subset of interaction terms using model selection criteria, such as **Akaike information criterion** (AIC) [46], **Bayesian information criterion** (BIC) [47], and cross-validation. First, for each model size, an AIC (or equivalent BIC, given fixed model size) was used to determine the best set of interactions to enter the model, while keeping in the model all the individual variables selected by the Lasso and some preselected interactions of particular interest. Then, we used a separate validation dataset to assess the model fit and chose the most appropriate model size based on the validation prediction errors.

2.5.4. Model Verification

After the 'best' model was determined, we checked the adequacy of the model for violation of linearity, variance homogeneity and normality. We performed residual analysis to identify outliers and removed those from the data with studentized residuals greater than 5. To be sure not to exclude observations that have studentized residuals falling between 3 and 5, which is a grey area when defining outliers, we also compared our regression model with two robust regression models. Robust regression is a procedure that is not sensitive to small deviations from the normal assumption of random errors and is often useful for confirming the reasonableness of the least squares regression

when suspicious outliers exist in the model. We considered robust regression models based on the Huber [48] and the Tukey bisquare estimators, respectively. Of the two estimators, the Tukey bisquare estimator is more robust and hence even less sensitive to the outliers.

As shown in Figure 2, the model development process was iterative and the final model was not picked until the model adequacy was verified and free of outliers. It is worth mentioning that in the very beginning of this model developing process, we partitioned the original data into 50% training data and 50% validation data. The models were trained from Section 2.5.1 to Section 2.5.4 using only the training set. The validation set only participated in selecting the optimal model size in the last step of Section 2.5.3. Hence, the validation set can be treated as a fairly independent dataset to evaluate model performance. In fact, in Section 2.5.4, we checked the model adequacy, including model fit, assumptions and outliers. We checked on both the training and validation sets for each considered model from the iterations. The final model was verified to have consistent performance across both the training and validation sets, which demonstrates final model robustness. After the final model was fit, to understand the relative importance of the explanatory variables, we also obtained the standardized coefficients, i.e., the coefficients for zero-centered and unit-scaled explanatory variables, and used them to determine which variables have a greater impact on the response, independent of their scale of units.

3. Results

3.1. Berlin Classification, Surface Temperature, GTLMPB

We found that 90% of the city area of Berlin can be explained with 19 STURLA classes. Three of the classes comprise one urban component and 16 are composite of multiple components. The surface temperature is lowest for the water-only class and in the combinations of trees, grass, and bare soil. It is warmer for composite classes that include components of the built environment. Figure 3 shows the 19 classes broken down by mean percent of within class composition and the mean surface temperature of grid cells in each class.

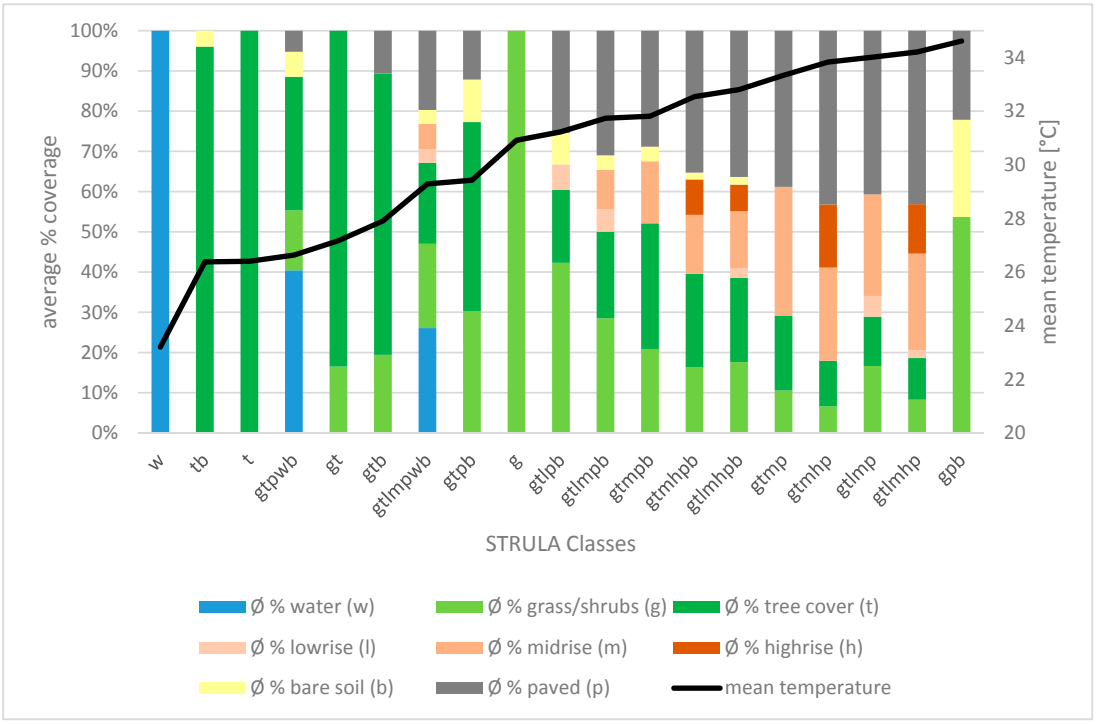

Figure 3. Mean surface temperature and percent land cover in Structure of Urban Landscape (STURLA) classes.

The 'GTLMPB' class comprises 35% of the total area of Berlin and can be found across the city with main concentrations outside the inner circle of the city center. The total land area of the 'GTLMPB' class is 326.5 sq km. Figure 4 shows the spatial distribution of GTLMPB and surface temperature in Berlin. The GTLMPB class has the largest temperature range of all Berlin STURLA classes 11.7–47.8 °C (1.95 STD).

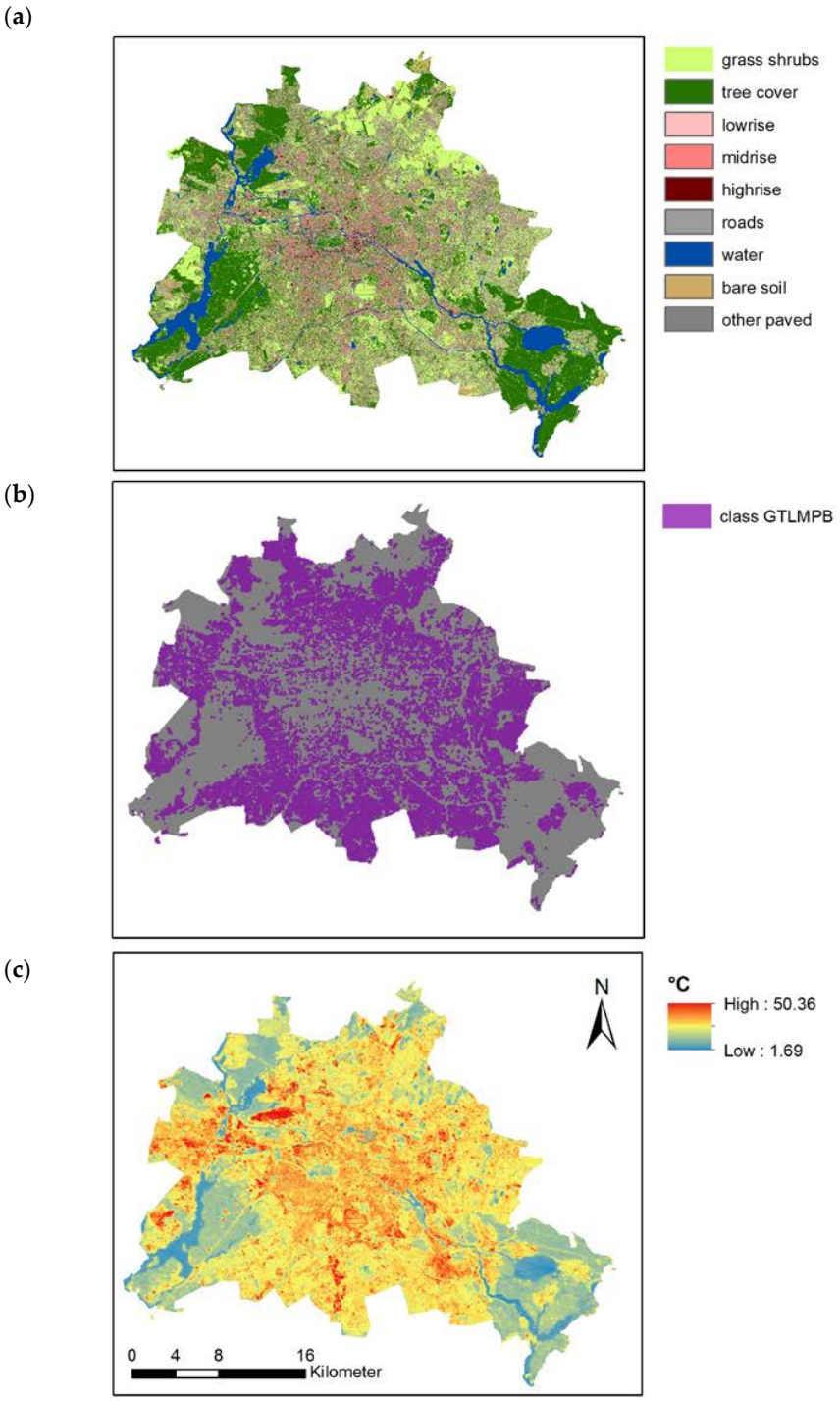

Figure 4. (**a**) Berlin land cover (above); (**b**) the distribution of Grass/Shrubs (g) –Tree Canopy (t) –Low-Rise (l) –Mid-Rise (m) –Roads-Other Paved (p) –Bare Soil (**b**) (GTLMPB) classes (middle) and; (**c**) surface temperature in Berlin (below).

3.2. Relationship between Surface Temperature, and Within-Class and Neighborhood Variables

Following the analysis in Section 2.5, the final model between surface temperature, and within-class and neighborhood variables, is given by:

$$\begin{aligned} 1/\hat{ST}^2 = \; & \hat{\beta}_0 + \hat{\beta}_{NH2}NH_2 + \hat{\beta}_{NH4}NH_4 + \hat{\beta}_{NH5}NH_5 + \hat{\beta}_{NH7}NH_7 + \hat{\beta}_{NH8}NH_8 + \hat{\beta}_{NH9}NH_9 \\ & + \hat{\beta}_{IC2}IC_2 + \hat{\beta}_{IC3}IC_3 + \hat{\beta}_{IC4}IC_4 + \hat{\beta}_{IC9}IC_9 \\ & + \hat{\beta}_{NH2*IC3}NH_2 \times IC_3 + \hat{\beta}_{NH4*IC3}NH_4 \times IC_3 + \hat{\beta}_{NH5*IC4}NH_5 \times IC_4 \\ & + \hat{\beta}_{NH2*NH8}NH_2 \times NH_8 + \hat{\beta}_{NH2*IC9}NH_2 \times IC_9, \end{aligned} \tag{4}$$

where $\hat{ST}$ is the estimated surface temperature; $\hat{\beta}_i$ is the coefficient of variable x_i and represents the change in $1/\hat{ST}^2$ per unit increase in x_i, holding all other explanatory variables $x_j (j \neq i)$ fixed.

The estimated coefficients in the models are given via **R** [49], output in Table 2.

Table 2. Coefficient estimates and model summary.

Coefficients	Estimate	Std. Error	*t* Value	*p*-Value	
(Intercept)	1.02×10^{-3}	4.01×10^{-6}	254.706	$<2 \times 10^{-16}$	***
NH_2	2.19×10^{-4}	1.35×10^{-5}	16.1923	$<2 \times 10^{-16}$	***
NH_4	-3.44×10^{-4}	1.95×10^{-5}	−17.603	$<2 \times 10^{-16}$	***
NH_5	-1.38×10^{-3}	1.02×10^{-4}	−13.476	$<2 \times 10^{-16}$	***
NH_7	1.61×10^{-4}	2.27×10^{-5}	7.07617	1.57×10^{-12}	***
NH_8	-2.71×10^{-4}	2.72×10^{-5}	−9.9629	$<2 \times 10^{-16}$	***
NH_9	-1.38×10^{-4}	1.53×10^{-5}	−9.0329	$<2 \times 10^{-16}$	***
IC_2	1.73×10^{-4}	8.80×10^{-5}	19.6777	$<2 \times 10^{-16}$	***
IC_3	2.32×10^{-5}	3.40×10^{-5}	0.68284	0.49472	
IC_4	-2.03×10^{-4}	1.33×10^{-5}	−15.254	$<2 \times 10^{-16}$	***
IC_9	-9.62×10^{-4}	1.41×10^{-5}	−6.8116	1.01×10^{-11}	***
NH_2 × IC_3	4.50×10^{-4}	1.36×10^{-4}	3.31257	0.00093	***
NH_4 × IC_3	-2.08×10^{-3}	2.12×10^{-4}	−9.8238	$<2 \times 10^{-16}$	***
NH_5 × IC_4	3.99×10^{-3}	4.85×10^{-4}	8.21461	2.36×10^{-16}	***
NH_2 × NH_8	2.00×10^{-3}	1.21×10^{-4}	16.5751	$<2 \times 10^{-16}$	***
NH_2 × IC_9	-4.15×10^{-4}	5.33×10^{-5}	−7.8006	6.71×10^{-15}	***

Signif. codes: 0 '***', 0.001 '**', 0.01 '*', 0.05 '.', 0.1 ' '; Residual standard error: 7.17×10^{-5} on 11,275 degrees of freedom ; Multiple R-squared: 0.653, Adjusted R-squared: 0.6525; F-statistic: 1414 on 15 and 11,275 DF, *p*-value: $< 2.2 \times 10^{-16}$.

Table 3 compares the standardized regression coefficients in the least squares model (our final model) and two robust regression models. Here, we standardized the coefficients in order to give a relatively fair assessment of how close the regression coefficients are between the three models.

From Table 3, the regression coefficients of our model and two robust regressions agreed quite well (in fact, all the differences are within two standard errors), except for the coefficients for the interaction NH_2 × NH_8 where the differences are above three standard errors. Although it is an open question which model gives the best estimated coefficient for NH_2 × NH_8, all three models rank NH_2 × NH_8 as the most important interaction predictor variable. Overall, the agreement between the three models reassures that our final model is a reasonable one, not unduly influenced by any observations with large deviations.

Then, we interpreted the results in the final model. Notice, since the response variable in model (1) was $1/ST^2$, if an explanatory variable yields a positive regression coefficient, it means that the corresponding urban component has the effect of reducing the surface temperature.

Table 3. Standardized regression coefficients of the least squares regression model versus two robust regression models.

Std. Coef.	Our Model	Robust_Huber	Robust_Bisquare
NH_2	2.98×10^{-5}	2.85×10^{-5}	2.76×10^{-5}
NH_4	-2.44×10^{-5}	-2.43×10^{-5}	-2.41×10^{-5}
NH_5	-1.54×10^{-5}	-1.53×10^{-5}	-1.54×10^{-5}
NH_7	4.87×10^{-6}	3.97×10^{-5}	3.66×10^{-6}
NH_8	-1.20×10^{-5}	-1.25×10^{-5}	-1.36×10^{-5}
NH_9	-1.14×10^{-5}	-1.15×10^{-5}	-1.22×10^{-5}
IC_2	2.81×10^{-5}	2.80×10^{-5}	2.78×10^{-5}
IC_3	1.15×10^{-6}	1.43×10^{-6}	1.51×10^{-6}
IC_4	-1.85×10^{-5}	-1.81×10^{-5}	-1.78×10^{-5}
IC_9	-1.10×10^{-5}	-1.16×10^{-5}	-1.11×10^{-5}
NH_2 × IC_3	4.34×10^{-6}	4.54×10^{-6}	4.46×10^{-6}
NH_4 × IC_3	-1.13×10^{-5}	-1.26×10^{-5}	-1.30×10^{-5}
NH_5 × IC_4	1.02×10^{-5}	8.96×10^{-6}	8.21×10^{-6}
NH_2 × NH_8	2.21×10^{-5}	2.67×10^{-5}	3.00×10^{-5}
NH_2 × IC_9	-1.02×10^{-5}	-9.64×10^{-6}	-1.01×10^{-5}

3.2.1. Main Effects

Individual components that are negatively related to surface temperature include within-class and neighborhood tree cover (IC_2; NH_2), and neighborhood water cover (NH_7). The variables that are positively related to surface temperature include within-class and neighborhood mid-rise buildings (IC_4; NH_4), neighborhood high-rise buildings (NH_5), neighborhood bare soil (NH_8) and within-class and neighborhood other paved surfaces (IC_9; NH_9). Note that the within-class low-rise buildings (IC_3) were kept in the model due to the presence of the related higher order terms, NH_2 × IC_3 and NH_4 × IC_3. However, the main effect of the within-class low-rise buildings is not significant (p-value = 0.49) in its association with surface temperature when holding other variables in the model constant.

The effects of the same component in within-class and neighborhood (i.e., within-class and neighborhood trees) typically respond similarly when related to surface temperature. However, some variables were only selected for the model in either within-class or neighborhood form. For example, bare soil is positively related to surface temperature in the within-class variable but the neighborhood variable was excluded by the Lasso method due to its weak association with surface temperature. Such is also the case for neighborhood low-rise buildings (NH_3); the within-class variable (IC_3) has turned insignificant in the model after interaction terms were added into the model. In addition, high-rise buildings and water cover are only represented as neighborhood variables because these components are not part of the GTLMPB class and hence not represented in within-class variables. Grass/Shrubs and roads were not selected for the model in either the within-class or neighborhood form, because of their low association with surface temperature and their high correlation with the other explanatory variables in the model.

3.2.2. Interaction Effects

The interactions between explanatory variables play an important role in the model. These interaction terms were selected by a combination of the authors' expertise and model selection techniques. The interactions involving neighborhood tree cover (NH_2) typically have an additional cooling effect, except for NH_2 × IC_9 (within-class paved). For example, when neighborhood tree cover (NH_2) and bare soil (NH_8) coexist, they will produce an extra cooling effect on temperature, in addition to their individual effects. On the contrary, when neighborhood tree cover is accompanied by the within-class paved component, the cooling effect of tree cover will be dampened by the interaction. Additionally, the presence of neighborhood high-rise (NH_5) around within-class mid-rise

(IC_4) produces an extra cooling effect on temperature, whereas neighborhood mid-rise (NH_4) and within-class low-rise (IC_3) exhibit an additional warming effect.

3.2.3. Variable Importance

Table 4 ranks the predictor variables in model (4) from most important to least important, based on the absolute values of their standardized coefficients in descending order.

Table 4. Variable importance from most important (top) to least important (bottom) based on standardized coefficients.

NH_2
IC_2
NH_4
NH_2 × NH_8
IC_4
NH_5
NH_8
NH_9
NH_4 × IC_3
IC_9
NH_2 × IC_9
NH_5 × IC_4
NH_7
NH_2 × IC_3
IC_3

From Table 4, the most important main effects on temperature reduction are tree cover in both local and neighborhood forms. Neighborhood and within-class mid-rise cover are the most important warming main effects. Neighborhood tree cover (NH_2) and bare soil (NH_8) are selected as the most important interaction effects and ranked 4th overall.

4. Discussion

In this paper, we aimed to answer two distinct questions raised by previous research: what is the relationship between class composition and surface temperature, and to what extent is surface temperature driven by the within-class components versus the importance of neighborhood effect on surface temperature? By asking these questions, we aim to continue to develop the STURLA classification system as a tool for analyzing commonly occurring urban building blocks and their relationship with ecological and environmental phenomena in cities.

In previous papers using the STURLA classification, it was demonstrated that classes created by the random application of a grid cell other than urban landscape can create meaningful composite classes and these can help explain the nuanced interaction between urban structure and surface temperature [11]. Examining the distribution of components within each STURLA cell and how such interactions impact surface temperature clarifies the relationships between urban components and surface temperature that drive these previous results. While STURLA classification was able to show a clear relationship with surface temperature on average, a main challenge with the methodology was the wide range of temperatures associated with certain classes, and particularly with highly mixed composite classes. For this reason, GTLMPB was chosen for this study. It is the most common class in Berlin, it is highly composite, and it encompasses the widest range of surface temperatures out of all STURLA classes. In addition, it is in the middle of the pack in terms of variance, and standard deviation (STD) values in this class are closer to the mean than (for example) values in the single component class of grass or the hyper composite class GTLMPWB.

As explained in the case study description, the mixture of built-up area and open space can be found everywhere in Berlin. Thus, it is not surprising that the most common class is a highly composite

one which can be found in all areas of the city. As illustrated in Figure 4, the class of GTLMPB can be found all over Berlin except from the very dense city center ("Berlin Mitte"), which is mainly characterized by high-rise and larger urban green spaces such as the Tiergarten. Closer to the city center, the class GTLMPB will be defined by the main components: mid-rise, paved, and low-rise (in this particular order), while with distance to the city center the share of grass/shrubs and tree canopy will increase and the share of mid-rise will gradually decrease.

Analyzing the GTLMPB class, we found that within-class and neighborhood variables, as well as the interaction between them, drive surface temperature. For within-class, our findings support common literature findings that particular urban components exert a strong influence on surface temperatures, both negative (e.g., trees) and positive (e.g., mid-rise buildings and paved surfaces). For example, Schwarz et al. [17] and Jenerette [21], like others, find vegetation (especially trees) to be associated with cooling, while paved surfaces are associated with warming at parcel and neighborhood scales. Our results indicate that local tree cover and neighborhood tree cover are the most important cooling components. In general, vegetation differs from the human made materials used in urban environments for their moisture and their aerodynamic and thermal properties [50]. The main process by which vegetation influences surface temperatures is evapotranspiration, in which plants use energy from solar radiation to evaporate water into the atmosphere. This process increases latent rather sensible heat and cools the leaf surface of plants and their immediate environment [51]. Trees provide another important mechanism—shade—by which cooling occurs. Tree shade reduced the storage and convection of heat on the surfaces that are covered by the tree canopy [52]. It is notable that, compared to tree cover, percent grass cover is not included in any of the final models, either at local or neighborhood scales. While in bivariate analysis, grass shows a negative association with surface temperature, grass becomes insignificant when other variables are considered. This may be attributed to the large variation in temperatures of grassy patches as exhibited in the grass only class. Moreover, the state of the grass cover depends on the soil properties, particularly its water holding capacity, which can be very distinct in urban areas and which makes different grass areas vary in their cooling effects [53]. In Berlin, many inner city grasslands were created at former rail brownfields with low quality sand or gravel-sand substrata, meaning that they present diminished capacity for cooling through evapotranspiration.

Neighborhood analysis was conducted to develop an understanding of the importance of the larger urban context in which composite classes are ingrained. It has been demonstrated in the existing literature that landscape configuration and context play an important role in the association with surface temperature [10,27,28]. In addition, preliminary findings from previous STURLA analysis indicate that neighborhood effects may partly explain the variation in the association of composite classes [12]. Results of this study confirm significant urban neighborhood effects on surface temperature. An increase in the percent of neighborhood green and water surrounding a composite class pixel contributed to a pixel's cooling while an increase in the percent of neighborhood mid-rise, high-rise, paved and bare soil contributes to a pixel's warming. Further research is required to determine the scale threshold of the neighborhood effects and whether they depend on the pure pixel size of the STURLA classification.

As expected, all paved and building components show a positive association with surface temperature. However, an important contribution of the STURLA approach is in the inclusion of the vertical dimension of the built environment, which enables the distinction between types of buildings and their urban context. Here, we find that different types of buildings show a significant difference in their association with surface temperature. Both neighborhood (overall rank 3) and within cell (rank 5) cover of mid-rise buildings are important warming components, followed by neighborhood high-rise buildings (rank 6). The importance of mid-rise and high-rise buildings in explaining surface temperature can be explained by the heightened capacity of buildings to uptake and retain heat not only because of the materials properties, but also due to reduced convective losses and ventilation, and by the additional warming due to trapping of radiation by vertical surfaces that

causes an increased absorption of solar radiation [16]. These findings provide empirical evidence supporting the need identified in the literature to address structure and architecture in studies of urban surface temperature [27] and more generally in the context of regulating urban ecosystem services [13]. Low-rise building cover was found to be significant only in its interactions with neighborhood tree cover and neighborhood mid-rise buildings. Results show that the presence of increasing neighborhood tree cover offers additional cooling, particularly in the case of low-rise buildings and in between paved surfaces. This can be explained by the effectiveness of trees in shading areas that are of similar or lower elevation.

The context in which low-rise occurs in Berlin is twofold. First, there are the classic detached or terrace housing areas, characterized by a low density, allocated in the peripheries of the city. Mostly, these detached and terrace houses have green or open spaces attached. Other pavement here occurs in the form of parking spaces, roads and sealed patios. Second, the other context refers to denser low-rise mixed with mid-rise and less green space, which occurs sometimes in the vicinity of high-rise, and is located closer to the inner city.

Interestingly, we find similar cooling effects in the interaction between neighborhood high-rise buildings and within class mid-rise buildings, further emphasizing the importance of artificial shading (through buildings) for surface temperature regulation. The contrary is seen in the interaction between within-class low-rise and neighborhood mid-rise, where a warming effect is compounded by the interaction. This is in accordance with recent findings by [54]. Finally, the strong cooling effect in the interaction between neighborhood tree cover and neighborhood bare soil indicates the importance of open space in urban structure.

5. Conclusions

The Structure of Urban Landscape classification offers a simple way to systematically classify urban areas into composite building blocks including land cover and building categories. In this paper we delved into the relationship between surface temperature and the composition of one such composite class, an urban building block common to Berlin: –grass/shrubs (g) –tree canopy (t) –low-rise (l) –mid-rise (m) –roads-other paved (p) –bare soil (b). We find that with-class composition as well as neighborhood composition and the interaction between them works to drive surface temperature. Our findings support the previously reported relationship between surface temperature and urban composition and structure and adds empirical evidence to a growing literature addressing the relationship between ecosystem services and complex urban structure. In this study, we confirm the importance of trees in cooling both local and neighborhood areas, and emphasize the importance of the urban context in which trees are present such as the effectiveness of trees in cooling low-rise buildings. Most importantly, we demonstrate the influence of the vertical dimension for surface temperature such as the warming effect of mid-rise building. Additional research is necessary to replicate these findings in different types of urban areas with different urban development histories, so as to test the utility of the STURLA classification in explaining other ecological and environmental processes, and in identifying the approaches' sensitivity to scale and orientation. Nonetheless, these findings, can support urban sustainability planning by providing insight for urban planners in considering the configuration of urban components when designing new development, rebuilding city centers and implementing urban ecological restoration.

Acknowledgments: The authors would like to thank five anonymous reviewers for their suggestions and help in improving the manuscript.

Author Contributions: Peleg Kremer, Neele Larondelle and Dagmar Haase conceived and designed the study, Peleg Kremer and Neele Larondelle collected and processed data and performed spatial analysis, Yimin Zhang and Elise Pasles performed statistical analysis. All authors contributed to writing.

Conflicts of Interest: The authors declare no conflict of interest.

Appendix A

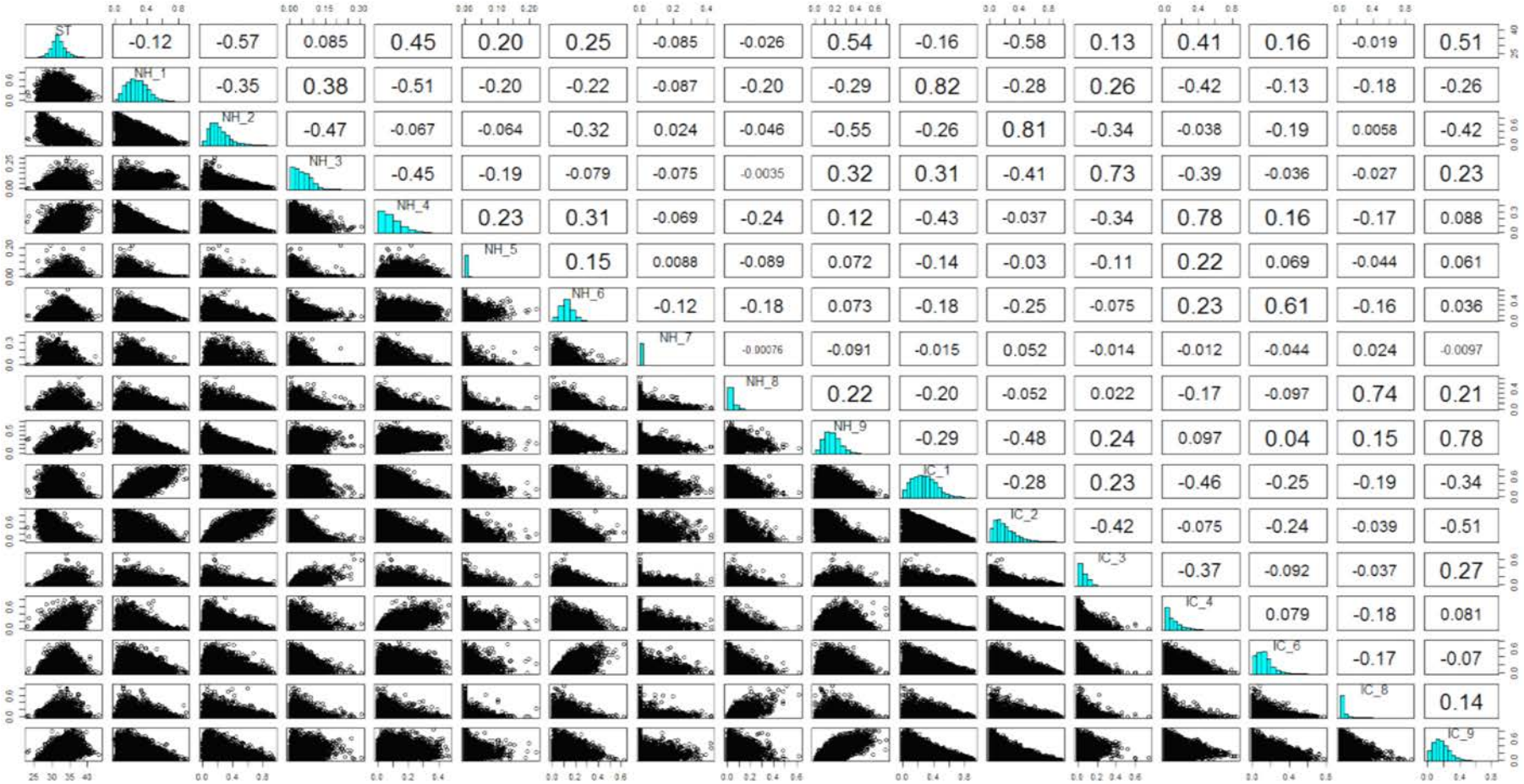

Figure A1. Scatterplot matrix of all variables.

References

1. UN-Habitat. *Planning Sustainable Cities: Global Report on Human Settlements 2009*; Earthscan: London UK, 2009; pp. 1–338.
2. Elmqvist, T.; Fragkias, M.; Goodness, J.; Güneralp, B.; Marcotullio, P.J.; McDonald, R.I.; Parnell, S.; Schewenius, M.; Sendstad, M.; Seto, K.C.; et al. (Eds.) *Urbanization, Biodiversity and Ecosystem Services: Challenges and Opportunities*; Springer: Dordrecht, The Netherlands, 2013.
3. McPhearson, T.; Pickett, S.T.; Grimm, N.B.; Niemelä, J.; Alberti, M.; Elmqvist, T.; Weber, C.; Haase, D.; Breuste, J.; Qureshi, S. Advancing Urban Ecology toward a Science of Cities. *Bioscience* **2016**, *66*, 198–212. [CrossRef]
4. Yigitcanlar, T.; Dizdaroglu, D. Ecological approaches in planning for sustainable cities. A review of the literature. *Glob. J. Environ. Sci. Manag.* **2015**, *1*, 159–188.
5. Zhou, W.; Pickett, S.T.A.; Cadenasso, M.L. Shifting concepts of urban spatial heterogeneity and their implications for sustainability. *Landsc. Ecol.* **2017**, *32*, 15–30. [CrossRef]
6. Bastian, O.; Grunewald, K.; Syrbe, R.-U.; Walz, U.; Wende, W. Landscape services: The concept and its practical relevance. *Landsc. Ecol.* **2014**, *29*, 1463–1479. [CrossRef]
7. Van Oudenhoven, A.P.E.; Petz, K.; Alkemade, R.; Hein, L.; de Groot, R.S. Framework for systematic indicator selection to assess effects of land management on ecosystem services. *Ecol. Indic.* **2012**, *21*, 110–122. [CrossRef]
8. Pickett, S.T.A.; Cadenasso, M.L. Linking ecological and built components of urban mosaics: An open cycle of ecological design. *J. Ecol.* **2008**, *96*, 8–12. [CrossRef]
9. Cadenasso, M.L.; Pickett, S.T.A.; Schwarz, K. Spatial heterogeneity in urban ecosystems: Reconceptualizing land cover and a framework for classification. *Front. Ecol. Environ.* **2007**, *5*, 80–88. [CrossRef]
10. Zhou, W.; Cadenasso, M.; Schwarz, K.; Pickett, S. Quantifying Spatial Heterogeneity in Urban Landscapes: Integrating Visual Interpretation and Object-Based Classification. *Remote Sens.* **2014**, *6*, 3369–3386. [CrossRef]
11. Hamstead, Z.A.; Kremer, P.; Larondelle, N.; McPhearson, T.; Haase, D. Classification of the heterogeneous structure of urban landscapes (STURLA) as an indicator of landscape function applied to surface temperature in New York City. *Ecol. Indic.* **2016**, *70*, 574–585. [CrossRef]
12. Larondelle, N.; Hamstead, Z.A.; Kremer, P.; Haase, D.; McPhearson, T. Applying a novel urban structure classification to compare the relationships of urban structure and surface temperature in Berlin and New York City. *Appl. Geogr.* **2014**, *53*, 427–437. [CrossRef]
13. Alavipanah, S.; Haase, D.; Lakes, T.; Qureshi, S. Integrating the third dimension into the concept of urban ecosystem services: A review. *Ecol. Indic.* **2017**, *72*, 374–398. [CrossRef]
14. Kaplan, S.; Peeters, A.; Erell, E. Predicting air temperature simultaneously for multiple locations in an urban environment: A bottom up approach. *Appl. Geogr.* **2016**, *76*, 62–74. [CrossRef]
15. Stewart, I.D.; Oke, T.R. Local climate zones for urban temperature studies. *Bull. Am. Meteorol. Soc.* **2012**, *93*, 1879–1900. [CrossRef]
16. Oke, T.R. The energetic basis of the urban heat island. *Q. J. R. Meteorol. Soc.* **1982**, *108*, 1–24. [CrossRef]
17. Schwarz, N.; Bauer, A.; Haase, D. Assessing climate impacts of planning policies-An estimation for the urban region of Leipzig (Germany). *Environ. Impact Assess. Rev.* **2011**, *31*, 97–111. [CrossRef]
18. Schwarz, N. Urban form revisited-Selecting indicators for characterising European cities. *Landsc. Urban Plan.* **2010**, *96*, 29–47. [CrossRef]
19. Zhang, X.; Li, P. A temperature and vegetation adjusted NTL urban index for urban area mapping and analysis. *ISPRS J. Photogramm. Remote Sens.* **2018**, *135*, 93–111. [CrossRef]
20. Trlica, A.; Hutyra, L.R.; Schaaf, C.L.; Erb, A.; Wang, J.A. Albedo, land cover, and daytime surface temperature variation across an urbanized landscape. *AGU Earth's Future* **2017**. [CrossRef]
21. Jenerette, G.D.; Harlan, S.L.; Buyantuev, A.; Stefanov, W.L.; Declet-Barreto, J.; Ruddell, B.L.; Myint, S.W.; Kaplan, S.; Li, X. Micro-scale urban surface temperatures are related to land-cover features and residential heat related health impacts in Phoenix, AZ USA. *Landsc. Ecol.* **2016**, *31*, 745–760. [CrossRef]
22. Weng, Q.; Lu, D.; Schubring, J. Estimation of land surface temperature-vegetation abundance relationship for urban heat island studies. *Remote Sens. Environ.* **2004**, *89*, 467–483. [CrossRef]
23. Rinner, C.; Hussain, M. Toronto's urban heat island-exploring the relationship between land use and surface temperature. *Remote Sens.* **2011**, *3*, 1251–1265. [CrossRef]

24. Yazhou, Z.; Yulin, Z.; Tao, Y.; Xinyu, R. Urban Green Effects on Land Surface Temperature Caused by Surface Characteristics: A Case Study of Summer Beijing Metropolitan Region. *Infrared Phys. Technol.* **2017**, *86*, 35–43.
25. Estoque, R.C.; Murayama, Y.; Myint, S.W. Effects of landscape composition and pattern on land surface temperature: An urban heat island study in the megacities of Southeast Asia. *Sci. Total Environ.* **2017**, *577*, 349–359. [CrossRef] [PubMed]
26. Buyantuyev, A.; Wu, J. Urban heat islands and landscape heterogeneity: Linking spatiotemporal variations in surface temperatures to land-cover and socioeconomic patterns. *Landsc. Ecol.* **2010**, *25*, 17–33. [CrossRef]
27. Li, X.; Li, W.; Middel, A.; Harlan, S.L.; Brazel, A.J.; Turner, B.L. Remote sensing of the surface urban heat island and land architecture in Phoenix, Arizona: Combined effects of land composition and configuration and cadastral-demographic-economic factors. *Remote Sens. Environ.* **2016**, *174*, 233–243. [CrossRef]
28. Connors, J.P.; Galletti, C.S.; Chow, W.T.L. Landscape configuration and urban heat island effects: Assessing the relationship between landscape characteristics and land surface temperature in Phoenix, Arizona. *Landsc. Ecol.* **2013**, *28*, 271–283. [CrossRef]
29. Zhou, W.; Huang, G.; Cadenasso, M.L. Does spatial configuration matter? Understanding the effects of land cover pattern on land surface temperature in urban landscapes. *Landsc. Urban Plan.* **2011**, *102*, 54–63.
30. Chen, A.; Yao, X.A.; Sun, R.; Chen, L. Effect of urban green patterns on surface urban cool islands and its seasonal variations. *Urban For. Urban Green.* **2014**, *13*, 646–654. [CrossRef]
31. Larondelle, N.; Haase, D. Urban ecosystem services assessment along a rural-urban gradient: A cross-analysis of European cities. *Ecol. Indic.* **2013**, *29*, 179–190. [CrossRef]
32. Larondelle, N.; Haase, D.; Kabisch, N. Mapping the diversity of regulating ecosystem services in European cities. *Glob. Environ. Chang.* **2014**, *26*, 119–129. [CrossRef]
33. Environmental Atlas of Berlin. *Digital Environmental Atlas: 01.02 Soil Sealing*; Senatsverwaltung für Stadtentwicklung: Berlin, Germany, 2012.
34. Environmental Atlas of Berlin. *Digital Environmental Atlas. 06.10 Building and Vegetation Height*; Senatsverwaltung für Stadtentwicklung: Berlin, Germany, 2014.
35. Larondelle, N.; Lauf, S. Balancing demand and supply of multiple urban ecosystem services on different spatial scales. *Ecosyst. Serv.* **2016**, *22*, 18–31. [CrossRef]
36. European Environmental Agency. Urban Atlas. 2012. Available online: http://land.copernicus.eu/local/urban-atlas/urban-atlas-2012/ (accessed on 5 November 2016).
37. Roy, D.P.; Ju, J.; Kline, K.; Scaramuzza, P.L.; Kovalskyy, V.; Hansen, M.; Loveland, T.R.; Vermote, E.; Zhang, C. Web-enabled Landsat Data (WELD): Landsat ETM+ composited mosaics of the conterminous United States. *Remote Sens. Environ.* **2010**, *114*, 35–49. [CrossRef]
38. Hu, L.; Brunsell, N.A. The impact of temporal aggregation of land surface temperature data for surface urban heat island (SUHI) monitoring. *Remote Sens. Environ.* **2013**, *134*, 162–174. [CrossRef]
39. Roy, D.P.; Ju, J.; Kommareddy, I.; Hansen, M.; Vermote, E.; Zhang, C.; Kommareddy, A. Algorithm Theoretical Basis Document Web Enabled Landsat Data (WELD). Available online: https://globalmonitoring.sdstate.edu/projects/weld/WELD_ATBD.pdf (accessed on 27 February 2018).
40. Sobrino, J.A.; Jiménez-Muñoz, J.C.; Paolini, L. Land surface temperature retrieval from LANDSAT TM 5. *Remote Sens. Environ.* **2004**, *90*, 434–440. [CrossRef]
41. Vlassova, L.; Perez-Cabello, F.; Nieto, H.; Martín, P.; Riaño, D.; la Riva, J.D. Assessment of methods for land surface temperature retrieval from landsat-5 TM images applicable to multiscale tree-grass ecosystem modeling. *Remote Sens.* **2014**, *6*, 4345–4368. [CrossRef]
42. Zareie, S.; Khosravi, H.; Nasiri, A. Derivation of land surface temperature from Landsat Thematic Mapper (TM) sensor data and analyzing relation between land use changes and surface temperature. *Solid Earth Discuss.* **2016**, 1–15. [CrossRef]
43. Box, G.E.; Cox, D.R. An analysis of transformations. *J. R. Stat. Soc. Ser. B* **1964**, *2*, 211–254.
44. Tibshirani, R. Regression Selection and Shrinkage via the Lasso. *J. R. Stat. Soc. B* **1996**, *58*, 267–288.
45. Marquardt, D.W. Generalized inverses, ridge regression, biased linear estimation, and nonlinear estimation. *Technometrics* **1970**, *12*, 591–612. [CrossRef]
46. Akaike, H. Information theory and an extension of the maximum likelihood principle. In *2nd International Symposium on Information Theory*; Akadémiai Kiadó: Budapest, Hungary, 1973.
47. Schwarz, G. Estimating the Dimension of a Model. *Ann. Stat.* **1978**, *6*, 461–464. [CrossRef]
48. Huber, P.J. *Robust Statistics*; John Wiley & Sons: Hoboken, NJ, USA, 1981; Volume 82.

49. R Core Team. *R: A Language and Environment for Statistical Computing*; R Foundation for Statistical Computing: Vienna, Austria, 2017.
50. Givoni, B. Impact of planted areas on urban environmental quality: A review. *Atmos. Environ. Part B Urban Atmos.* **1991**, *25*, 289–299. [CrossRef]
51. Bowler, D.E.; Buyung-Ali, L.; Knight, T.M.; Pullin, A.S. Urban greening to cool towns and cities: A systematic review of the empirical evidence. *Landsc. Urban Plan.* **2010**, *97*, 147–155. [CrossRef]
52. Armson, D.; Stringer, P.; Ennos, A.R. The effect of tree shade and grass on surface and globe temperatures in an urban area. *Urban For. Urban Green.* **2012**, *11*, 245–255. [CrossRef]
53. Haase, D. Effects of urbanisation on the water balance—A long-term trajectory. *Environ. Impact Assess. Rev.* **2009**, *29*, 211–219. [CrossRef]
54. Alavipanah, S.; Schreyer, J.; Haase, D.; Lakes, T.; Qureshi, S. The effect of multi-dimensional indicators on urban thermal conditions. *J. Clean. Prod.* **2018**, *177*, 115–123. [CrossRef]